

# Entanglement, Elasticity and Viscous Relaxation of Actin Solutions

B. Hinner\*, M. Tempel\*, E. Sackmann\*, K. Kroy#, E. Frey#,§

\*Institut E22, Biophysik, #Institut für Theoretische Physik, Technische Universität München, James-Franck-Straße, 85747 Garching, Germany; §present address: Physics Department, Harvard University, Cambridge, MA 02138

We have investigated the viscosity and the plateau modulus of actin solutions with a magnetically driven rotating disc rheometer. For entangled solutions we observed a scaling of the plateau modulus versus concentration with a power of 7/5. The measured terminal relaxation time increases with a power 3/2 as a function of polymer length. We interpret the entanglement transition and the scaling of the plateau modulus in terms of the tube model for semiflexible polymers.

Networks of semiflexible macromolecules are major constituents of biological tissue. There is experimental evidence [1–4] that certain aspects of biologically important macromolecules, such as DNA and actin, are well described by the minimal theoretical model of a semiflexible macromolecule, also known as the *wormlike chain* model. This model represents the polymer as a smooth inextensible contour with an energy cost for bending and includes ideal flexible chains as a limiting case. The bending modulus of the single molecule can be expected to be constitutive also for the *collective* mechanical properties of gels and sufficiently concentrated solutions of semiflexible polymers. (Recently, possible contributions from twist have also been discussed [5].) However, very little is known about how semiflexible polymers build up statistical networks, and how the macroscopic stresses and strains are mediated to the single molecules in such networks. This is also known as the *entanglement problem*. In this Letter, we report on experiments performed with a magnetically driven rotating disc rheometer, which elucidate some important aspects of the entanglement problem. The systems under scrutiny are *in vitro* polymerized actin solutions of various concentrations  $c$  and average polymer lengths  $L$ . Actin [6] forms large semiflexible polymers with a persistence length  $\ell_p$  of about 17  $\mu\text{m}$  [7,8] (comparable to typical filament lengths in our experiments), and is the most abundant cytoskeletal element in most eukaryotic cells. We have analyzed the transition from the dilute to the semidilute phase (the entanglement transition) as a function of polymer length and concentration. The data can be interpreted in terms of a virial expansion for effective “tubes”. For entangled solutions we observed a scaling of the plateau modulus  $G^0$  versus actin concentration  $c$ . This is compared with various theoretical predictions [9–14]. Lastly, we analyzed the dependence of the zero shear rate viscosity on polymer length, which exhibits a much weaker length dependence than one would expect theoretically from work by Odijk [9] and Doi [15].

Actin was prepared as previously described [16], and purified in a second step using gel column chromatography (Sephadex S-300). Monomeric actin (called G-

actin) was kept in G-buffer, consisting of 2 mM Imidazol (pH 7.4), 0.2 mM  $\text{CaCl}_2$ , 0.2 mM DTT, 0.5 mM ATP, and 0.005 vol%  $\text{NaN}_3$ . Polymerization was initiated by adding 1/10 of the sample volume of 10-fold concentrated F-buffer containing 20 mM Imidazol (pH 7.4), 2 mM  $\text{CaCl}_2$ , 1 M KCl, 20 mM  $\text{MgCl}_2$ , 2 mM DTT, and 5 mM ATP. Gelsolin was prepared from bovine plasma serum according to Ref. [17], and stored dissolved in G-buffer at 4°C for several weeks. The purity of the proteins was checked by SDS-PAGE electrophoresis. After staining with coomassie blue [18] only one single band was detected. The mean length of actin filaments was adjusted by adding gelsolin to G-actin before initiating polymerization. According to results by Janmey *et al.* [19] we computed the average actin length from the molar ratio  $r_{\text{AG}}$  of actin to gelsolin as  $L [\mu\text{m}] = r_{\text{AG}}/370$ . All measurements were done at room temperature ( $20 \pm 0.1$ )°C. Both oscillatory and creep experiments were performed with a magnetically driven rotating disc rheometer, as described previously [16]. Care was taken to keep the strain below 1% to probe linear response. For oscillatory measurements the phase shift between exciting force and observed oscillation and the response amplitude were recorded. From these two parameters the dynamic storage and loss modulus (real and imaginary part of the stress amplitude divided by the strain amplitude) were obtained for frequencies  $\omega/2\pi = 10^{-4}$  to  $10^1$  Hz. The creep compliance  $J(t)$  was obtained for times  $t = 10^{-1}$  to  $10^4$  s by applying a sudden step force to the sample and recording its strain, which is proportional to  $J(t)$ . In both cases the apparatus was calibrated with purely viscous liquids of known viscosities. A quantitative measure for the elastic character of a material is the phase shift. In the limiting case of a purely elastic medium the phase shift is zero, in the opposite case of a purely viscous liquid the phase shift is  $\pi/2$ . Consequently, the sample behaves most rubber-like when the phase shift becomes minimal. Therefore, in oscillatory experiments with actin/gelsolin the value of the storage modulus at the frequency corresponding to the minimum phase shift was identified as the *plateau modulus*  $G^0$ . For actin samples without gelsolin, where no minimum in the phase could be observed

within the measured frequency range, the storage modulus at a fixed frequency in the plateau regime was taken as  $G^0$ . This does not affect the functional form of  $G^0(c)$  but its absolute value. (As a consequence, the vertical shift between the two data sets shown in Fig. 3 has no physical significance.) For the circles in Fig. 2,  $G^0$  was determined by the minimum phase prescription at the highest concentration only, whereas relative shifts of  $G^0$  at lower concentrations were determined by rescaling to superimpose the moduli. The *zero shear rate viscosity*  $\eta_0$  was obtained from measurements of the creep compliance  $J(t)$  according to  $\eta_0^{-1} := \lim_{t \rightarrow \infty} J(t)/t$  [20]. From creep experiments we extracted the frequency dependent moduli (to obtain  $G^0$  for Fig. 1) as described in Ref. [21]. It was checked that the results agree well with corresponding oscillatory measurements [21].

Figs. 1, 2, and 3 show the plateau modulus  $G^0$  as a function of filament length  $L$  and actin concentration  $c$ , respectively. The data in Fig. 1 clearly indicate a transition with increasing length of polymers. Similar results also have been obtained by Janmey *et. al.* [22], recently. At first sight, one might be tempted to attribute this transition to the mutual steric hindrance in a solution of *rods* at the overlap concentration. The observed transition is indeed in a parameter regime, where the polymer length  $L$  is not much larger (about a factor of 5) than the mesh size  $\xi_m$ , and we originally attempted to interpret the data this way. Some more thought suggests, however, that there is no transition expected for the plateau modulus of stiff rods; a sudden increase in the shear modulus near the overlap concentration would not be in accord with the virial expansion for the osmotic pressure of rods [23], which predicts a smooth dependence on  $c$  and  $L$  below the nematic transition. One can hardly imagine the shear modulus of a semidilute solution of rods to be larger than the osmotic compression modulus. The solution could easily escape the shear stress by local compression. On the other hand, the actin solutions in our experiments were below the critical concentration for the nematic transition [24,25]. We can thus conclude that the observed sudden increase (Fig. 1), and the enhanced concentration dependence (Fig. 2, 3) of  $G^0$  above a certain threshold are related to the semiflexible nature of actin filaments. Their persistence length of about  $17 \mu\text{m}$  [7,8], albeit much larger than the typical mesh size  $\xi_m \simeq 0.1 - 1 \mu\text{m}$  of the studied networks, can not be assumed to be infinitely large. Otherwise the data would have to obey the prediction of the classical theory for dilute and semidilute rods [26].

$$G^0 = 3\nu k_B T/5. \quad (1)$$

Here  $\nu = 3/\xi_m^2 L$  is the polymer number density. It is not conceivable that the sudden steep increase of  $G^0$  with polymer length is merely due to internal modes of *single* polymers neglected in the theory for stiff rods. Instead we are forced to look for a *cooperative effect*.

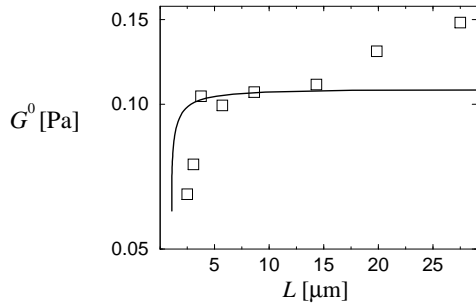


FIG. 1. The plateau modulus above the entanglement transition as a function of polymer length for constant monomeric actin concentration  $c = 1.0 \text{ mg/ml}$ . The solid line corresponds to Eq. (2) with  $\xi_1 = 0.38$ . The increase of  $G^0$  for large  $L$  is not yet fully understood.

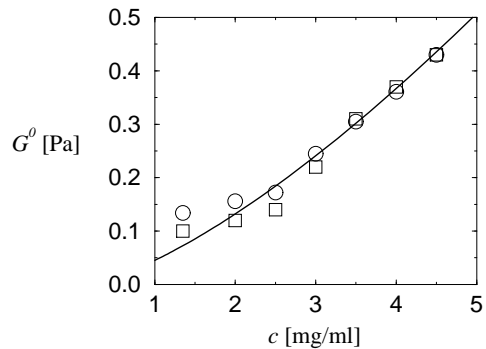


FIG. 2. The plateau modulus near the entanglement transition as a function of polymer concentration for short rod-like actin filaments ( $L = 1.5 \mu\text{m}$ ). Two different methods were used to extract  $G^0$  from the data (see main text). Also shown is the theoretical prediction, Eqs. (2) for  $\xi_1 = 0.47$ . Theoretically the transition is expected at  $c^* = 0.68 \text{ mg/ml}$ .

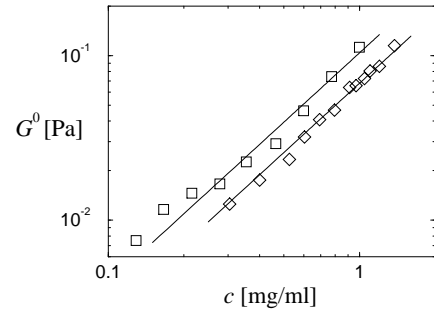


FIG. 3. Concentration dependence of the plateau modulus of pure actin (□) and actin with a small amount of gelsolin ( $r_{\text{AG}} = 6000 : 1$ ) corresponding to an average actin filament length  $L = 16 \mu\text{m}$  (◇). The straight lines indicate the power  $7/5$  corresponding to the scaling limit of Eq. (2) with  $\xi_1 = 0.40$  and  $\xi_1 = 0.46$ , respectively.

In the following we attempt to give a simple interpretation of our observations based on the tube concept for

semiflexible polymers developed theoretically by Odijk [9] and Semenov [10] and related to the shear modulus by Isambert and Maggs [12], recently. Experimentally, it has been demonstrated by video-microscopy that in semidilute actin solutions the filaments are confined to tube-like cages [27]. These cages severely hinder not only transverse and rotational motions but also undulations on length scales larger than a certain length  $L_e$ , called *deflection length* or *entanglement length*. Using the wormlike chain free energy one can relate  $L_e$  to the tube diameter  $d$  by  $L_e^3 = \sqrt{2}d^2\ell_p$  [9,28]. On the time scale of the plateau, modes of wavelength smaller than  $L_e$  are already equilibrated. Hence, on this coarse grained time scale we can think of the polymer solution in terms of an ensemble of tubes. If we apply a reasoning similar to that used for the osmotic pressure of dispersed rods [23] to the plateau modulus of *dispersed tubes* of length  $L$  and diameter  $d$ , we can replace Eq. (1) by a virial expansion

$$G^0 = (3/5)\nu k_B T(1 + 2B_2\nu \dots) . \quad (2)$$

Here,  $B_2$  is the second virial coefficient for the tubes. Higher order terms are negligible for small volume fraction of the tubes. (The latter turns out to be less than 0.1 in our case.) The product  $B_2\nu$  counts the average number of collisions of the tubes, and can thus be used to define a collision length  $L_c := L/2B_2\nu$  (always two tubes are involved in a collision). According to Ref. [23] the second virial coefficient is given by the excluded volume  $B_2 = \pi dL^2/4$  of a tube. However, to stay consistent with our assumption that short wavelength modes have already relaxed, we subtract from  $L$  half the collision length at each end to account for the reduced efficiency of dangling ends in the entanglement process. The above relation between the second virial coefficient and the collision length thus becomes

$$L/L_c - 1 = \pi\nu d(L - L_c)^2/2 . \quad (3)$$

We can determine the still unknown tube diameter  $d$  from the following consistency requirement. Following Onsager's argument for the second virial coefficient we have to pay a price in free energy of the order of  $k_B T$  per length  $L_c$  to add a new tube to the solution. On the other hand, to suppress thermal undulations of wavelengths larger than  $L_e$  the tube has to supply a confinement energy of the order  $k_B T L_e$  to the enclosed polymer. Now, if we want the tube to be a pertinent effective representation of the medium surrounding a test polymer in the entangled polymer solution, these two energies should be equal. We do not actually have to introduce a physical tube into the solution when adding a polymer. Hence, for consistency we require  $L_c \equiv L_e$ , i.e., the number of mutual collisions of the tubes must equal the number of collisions of the polymers with their tubes. For entangled solutions we thus find  $G^0 = 9k_B T/5\xi_m^2 L_e$ , where far from the entanglement transition  $L_e$  and  $d$  take their asymptotic val-

ues  $L_e \approx 0.58\xi_m^{4/5}\ell_p^{1/5}$  and  $d \approx 0.37\xi_m^{6/5}\ell_p^{-1/5}$ . The scaling behavior was predicted by Isambert and Maggs [12] from a different reasoning before. We also note that it is included as a limiting case in a more detailed analysis concerned with the calculation of the absolute value of  $G^0$  [29]. The corresponding scaling  $G^0(c) \propto c^{7/5}$  of the plateau modulus is indicated by the solid lines in Fig. 3. A much stronger concentration dependence – as predicted by a purely mechanical model [13] or by a model with thermodynamic buckling [11] – and the scaling predicted in [14] are not in accord with our data. On the other hand, the agreement of Eq. (2) with the data seems to hold beyond the scaling limit of strong entanglement. To relate the apparent (theoretical) volume fraction to the nominal experimental actin concentration  $c$  we introduce the symbol  $\xi_1$  for the apparent mesh size  $\xi_m$  [ $\mu\text{m}$ ] of a solution with  $c = 1 \text{ mg/ml}$ . Solving Eq. (3) we predict the entanglement transition to occur at a concentration  $c^* \text{ [mg/ml]} = 7 \cdot 2^{1/4}\ell_p^{1/2}\xi_1^2/3\pi(5L/7)^{5/2}$  (weakly bending rod limit assumed). The critical concentration is thus theoretically by a factor of  $c^*/\bar{c} \approx 2.0(\ell_p/L)^{1/2}$  larger than the overlap concentration  $\bar{c}$ . For the persistence length we assumed  $\ell_p = 17 \mu\text{m}$  [7,8] for all our fits. The only free parameter of the theoretical curves in Figs. 1, 2, and 3 is thus  $\xi_1$ . It was chosen as  $\xi_1 = 0.38$  for Fig. 1,  $\xi_1 = 0.47$  for Fig. 2, and  $\xi_1 = 0.40/0.46$  for the upper/lower line in Fig. 3, in reasonable agreement with the value  $\xi_1 = 0.35$  obtained independently by FRAP (fluorescence recovery after photo bleaching) [30]. The scatter in the value for  $\xi_1$  merely reflects the poor experimental reproducibility of absolute values of  $G^0$  for F-actin solutions.

Simultaneously with the length dependence of the plateau modulus shown in Fig. 1, we have measured the length dependence of the zero shear rate viscosity  $\eta_0$ . The latter is partly due to static effects, namely the length dependence of the plateau modulus discussed above, and also to dynamics. The *terminal relaxation time*  $\tau_r$ , the characteristic time scale at which a polymer solution begins to flow, can be obtained up to a numerical coefficient from the viscosity via  $\tau_r \simeq \eta_0/G^0$ . Fig. 4 presents such data on the length dependence of  $\tau_r$ . Data (not shown) obtained directly from the frequency dependent viscoelastic moduli by the condition  $G'(2\pi/\tau_r) = G^0/2$  or by  $\partial G''(2\pi/\tau_r)/\partial\omega = 0$  fall onto the same curve if multiplied by numerical prefactors 1.0 and 2.4 [21], respectively. The mechanism for the terminal relaxation seems obvious from the tube picture described above. Viscous relaxation only occurs when the polymers have time to leave their tube-like cages by Brownian motion along their axis. The reptation model that was originally formulated for flexible polymers, was extended to semiflexible chains by Odijk [9] and Doi [15]. These authors calculated the disengagement time  $\tau_d$  for a semi-flexible chain diffusing out of its tube. However, the

data for  $\tau_r$  presented in Fig. 4 are not in accord with their result for  $\tau_d$ . The dependence of the observed terminal relaxation time  $\tau_r$  on polymer length  $L$  is substantially weaker than predicted for  $\tau_d$ , even in the stiff limit where  $\tau_d = \ell_p L / 4D_{\parallel} \propto L^2$  (dot-dashed line in Fig. 4),  $D_{\parallel} = k_B T / 2\pi\eta L$  being the longitudinal diffusion coefficient of the chain in the free draining approximation. Instead, the solid line in Fig. 4 corresponds to the scaling law  $\tau_r \propto L^{3/2}$ .

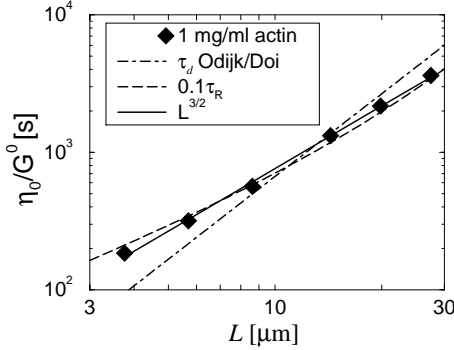


FIG. 4. Terminal relaxation time in the entangled phase for constant actin concentration  $c = 1.0$  mg/ml. The solid line indicates the power 3/2 and the dashed line is Eq. (4) with a numerical prefactor of 0.10. The dot-dashed line is the disentanglement time calculated by Odijk and Doi [9,15].

A tentative interpretation of the data can be given in terms of a semiflexible polymer diffusing along a strictly one dimensional path; i.e., not being allowed to choose between infinitely many new directions at its ends. The characteristic decay time for self-correlations of the end-to-end vector  $\langle \mathbf{R}(t)\mathbf{R} \rangle$  is then given by [28]

$$\tau_R = L^4 \ell_p^2 / D_{\parallel} \langle R^2 \rangle^2 \approx (L + 2\ell_p)^2 / 4D_{\parallel}. \quad (4)$$

This presents an upper bound for the terminal relaxation time within the tube model. As seen from the dashed line in Fig. 4,  $\tau_R$  (for  $\ell_p = 17 \mu\text{m}$ ) is in fact by a factor of ten too large compared to the data but describes fairly well the length dependence of  $\tau_r$ . The restriction to one path implies a very slow decay of conformational correlations [28]. An unusually slow decay of stress (the frequency dependence of  $G'(\omega)$  is still less than linear in the measured frequency range) is indeed observed, but this might also in part be due to the broad length distribution of actin [19]. Clearly, further investigations are necessary to come to a better understanding of the terminal regime.

In summary, we were able to measure some important physical properties of semiflexible polymer solutions with a rotating disc rheometer. We investigated the plateau modulus and the zero shear rate viscosity of semidilute actin solutions. At a certain concentration  $c^*$  larger than the overlap concentration  $\bar{c}$  an increase in the plateau modulus was observed. We interpreted this entanglement transition as well as the concentration dependence of the

plateau modulus in terms of a tube model that takes into account the semiflexible nature of the molecules. For strongly entangled solutions our data can be characterized by the scaling law  $G^0 \propto c^{7/5}$ . We also found a power law dependence of the terminal relaxation time on polymer length  $\tau_r \propto L^{3/2}$ , which is substantially weaker than predicted for the disengagement time by Odijk and Doi.

This work was supported by the Deutsche Forschungsgemeinschaft under Contract No. SFB 266. E. F. acknowledges support by a Heisenberg fellowship (FR 850/3-1). We thank J. Wilhelm for helpful discussions and suggestions, M. Bärmann for critical comments, B. Wagner (Fraunhofer-Institut für Siliziumtechnologie, Berlin) for the micro-magnets of the rheometer, and our biochemistry laboratory for preparing the proteins.

---

- [1] S. B. Smith, L. Finzi, and C. Bustamante, *Science* **258**, 1122 (1992).
- [2] R. Götter *et al.*, *Macromol.* **29**, 30 (1996).
- [3] F. Amblard *et al.*, *Phys. Rev. Lett.* **77**, 4470 (1996).
- [4] D. Riveline, C. H. Wiggins, R. E. Goldstein, and A. Ott, *Phys. Rev. E* **56**, R1330 (1997).
- [5] A. C. Maggs, *Phys. Rev. E* **55**, 7396 (1997).
- [6] J. Käs *et al.*, *Biophys. J.* **70**, 609 (1996).
- [7] A. Ott, M. Magnasco, A. Simon, and A. Libchaber, *Phys. Rev. E* **48**, R1642 (1993).
- [8] F. Gittes, B. Mickey, J. Nettleton, and J. Howard, *Journal of Cell Biology* **120**, 923 (1993).
- [9] T. Odijk, *Macromol.* **16**, 1340 (1983).
- [10] A. N. Semenov, *J. Chem. Soc. Faraday Trans.* **86**, 317 (1986).
- [11] F. MacKintosh, J. Käs, and P. Janmey, *Phys. Rev. Lett.* **75**, 4425 (1995).
- [12] H. Isambert and A. C. Maggs, *Macromol.* **29**, 1036 (1996).
- [13] R. L. Satcher, Jr. and C. F. Dewey, Jr., *Biophys. J.* **71**, 109 (1996).
- [14] K. Kroy and E. Frey, *Phys. Rev. Lett.* **77**, 306 (1996).
- [15] M. Doi, *J. Pol. Sci. Pol. Symp.* **73**, 93 (1985).
- [16] M. Tempel, G. Isenberg, and E. Sackmann, *Phys. Rev. E* **54**, 1802 (1996).
- [17] J. A. Cooper *et al.*, *J. Cell. Biol.* **104**, 491 (1987).
- [18] U. K. Laemmlli, *Nature* **227**, 680 (1970).
- [19] P. A. Janmey *et al.*, *J. Biol. Chem.* **261**, 8357 (1986).
- [20] K. Ninomiya, *J. Phys. C* **67**, 1152 (1963).
- [21] M. Tempel, Ph.D. thesis, TU München, 1996.
- [22] P. A. Janmey *et al.*, *J. Biol. Chem.* **269**, 32503 (1994).
- [23] L. Onsager, *Ann. N. Y. Acad. Sci.* **51**, 627 (1949).
- [24] A. Suzuki, T. Maeda, and T. Ito, *Biophys. J.* **59**, 25 (1991).
- [25] C. M. Coppin and P. C. Leavis, *Biophys. J.* **63**, 794 (1992).
- [26] M. Doi and S. F. Edwards, *The Theory of Polymer Dynamics* (Clarendon Press, Oxford, 1986).

- [27] J. Käs, H. Strey, and E. Sackmann, *Nature* **368**, 226 (1994).
- [28] K. Kroy, Ph.D. thesis, TU München, 1998.
- [29] J. Wilhelm and E. Frey (unpublished).
- [30] C. Schmidt, M. Bärmann, G. Isenberg, and E. Sackmann, *Macromol.* **22**, 3638 (1989).